World Academy of Science, Engineering and Technology
International Journal of Aerospace and Mechanical Engineering
Vol:10, No:12, 2016

# Numerical Study of Flapping-Wing Flight of Hummingbird Hawkmoth during Hovering: Longitudinal Dynamics

Yao Jie, Yeo Khoon Seng



***Abstract*****—**In recent decades, flapping wing aerodynamics has attracted great interest. Understanding the physics of biological flyers such as birds and insects can help improve the performance of micro air vehicles. The present research focuses on the aerodynamics of insect-like flapping wing flight with the approach of numerical computation. Insect model of hawkmoth is adopted in the numerical study with rigid wing assumption currently. The numerical model integrates the computational fluid dynamics of the flow and active control of wing kinematics to achieve stable flight. The computation grid is a hybrid consisting of background Cartesian nodes and clouds of mesh-free grids around immersed boundaries. The generalized finite difference method is used in conjunction with single value decomposition (SVD-GFD) in computational fluid dynamics solver to study the dynamics of a free hovering hummingbird hawkmoth. The longitudinal dynamics of the hovering flight is governed by three control parameters, i.e., wing plane angle, mean positional angle and wing beating frequency. In present work, a PID controller works out the appropriate control parameters with the insect motion as input. The controller is adjusted to acquire desired maneuvering of the insect flight. The numerical scheme in present study is proven to be accurate and stable to simulate the flight of the hummingbird hawkmoth, which has relatively high Reynolds number. The PID controller is responsive to provide feedback to the wing kinematics during the hovering flight. The simulated hovering flight agrees well with the real insect flight. The present numerical study offers a promising route to investigate the free flight aerodynamics of insects, which could overcome some of the limitations of experiments.

***Keywords*****—**Aerodynamics, flight control, computational fluid dynamics, flapping-wing flight.

## I. Introduction

INSECTS represent some of the most versatile and manoeuvrable flying animals. Many of them can hover, take off backwards, decelerate rapidly, and some insects can even land upside down. This kind of rapid energy-efficient flight has permitted access to more abundant ecological resources and rapid escape from predators. The remarkable capacity for mobility and manoeuvrability in air has greatly interested biologists, scientists and engineers to study and understand the physical phenomenon of insect flight, which can play key role in improving Micro Air Vehicle (MAV) design. Yet, insects cannot generate enough lift to fly in the sense of conventional laws of aerodynamics, which rely on steady state approximations. The extra lift required must be generated from the complex (unsteady) flapping motions generated during the wing-flapping cycle [1]. Until recently, the exact nature of this extra source of lift remains a mystery. By understanding the aerodynamics associated with insect flight, a new lift generation system can be developed, which would be a great breakthrough in aerodynamics.

Experimental biomechanics and fluid dynamics have played a key role in the study of flapping flight for a long time. Experiment has its limitation in understanding the physics of flapping flight due to the difficulty in observing wing kinematics with small physical scales, visualizing unsteady flow with great complexity and controlling test subjects with desired motion [2], [3]. The Computational Fluid Dynamics (CFD) has offered a more convenient and affordable approach for the unsteady aerodynamic study. Benefiting from the continuously improving computing hardware and technology, the development of CFD has advanced rapidly in the past several decades. A diverse variety of numerical schemes have been developed to assist in the study of aerodynamics in aviation, automobile, marine engineering, environmental engineering and many other industrial and research areas [4], [5].

CFD tools are widely available in standard software packages such as Fluent, CFX, Star-CD, etc. now for both industrial and scientific applications. These standard software packages show reliability and convenience in common fluid flow problems especially for steady flow problems. The complex kinematics of flapping wing motion makes it necessary to use moving mesh or other re-meshing methods to resolve mesh deformation problem [6]. In addition, the rigid body motion has to be solved together with the flow field when controlled flight is involved. Since most of the software packages have adopted only Eularian methods, they are not suitable for immersed boundary problems, especially when the boundary has complicated motion. This indicates that current standard software packages have inherent drawbacks for solving flapping flight problems, such as poor numerical accuracy and high computation cost.

Singular Value Decomposition based Generalised Finite Difference (SVD-GFD) is a novel numerical scheme that was continually developed in the Department of Mechanical Engineering, National University of Singapore. This numerical scheme is capable of achieving high numerical accuracy in solving for complex immersed boundary (IB) problems with

Yao Jie, Yeo Khoon Seng are with the National University of Singapore, 119077, Singapore (e-mail: yaojie@u.nus.edu).

improved computational efficiency as compared to the generally adopted Finite Element and Finite Volume methods in solving such problems [7]-[9].

The purpose of the current research work is to use the aforementioned CFD scheme to simulate and study insect flapping flight problems and attempt to gain understanding of the unsteady aerodynamics involved in flapping wing flights and maneuvering.

## II. Methodology

Insect models are used in current numerical simulations. Hummingbird hawkmoth (*Macroglossum stellatarum*) is adopted as the model flapping wing flyer with relatively high Reynolds number (Fig. 1).

Fig. 1 Hummingbird hawkmoth (*Macroglossum stellatarum*)

The flapping wing motion of hummingbird hawkmoth has a frequency $f$ of approximately 70 Hz and a stroke amplitude $\Phi$ of about 115° according to literature [10]. The Reynolds number of the flyer with a reference length of wing mean chord $\bar{c}$ and a reference velocity of wing tip $U_{ref}$ is

$$\mathrm{Re} = \frac{\bar{c}U_{\mathrm{ref}}}{\nu} = \frac{\bar{c} \cdot R \cdot 2\Phi \cdot f}{\nu} = \frac{4R^2 \Phi f}{\nu \cdot AR} \tag{1}$$

where $\nu = 1.5\times10^{-5}$ m$^2$·s$^{-1}$ is the kinematic viscosity of air, $AR = (2R)^2/S$ is the aspect ratio with the surface area of a wing pair $S = 2R\bar{c}$. The Reynolds number thus works out to be around 3000, which is much higher than that of fruit fly (148) [6].

The flyer's geometric model is shown in Fig. 2 with global coordinate $(x, y, z)$ and insect body coordinate $(x, y, z)^b$. The insect model is created with a pre-set pitch angle of 45° in the body coordinate system; because a hummingbird hawk moth hovers with body pitch approximately that angle. The body coordinate is aligned with the global coordinate initially, which is also the hovering equilibrium position.

The governing equation of fluid flow in insect flapping flight problems is the three-dimensional incompressible Navier-Stokes equations, given in the non-dimensional Arbitrary Lagrangian-Eulerian (ALE) form:

$$\nabla \cdot \mathbf{u} = 0 \tag{2}$$

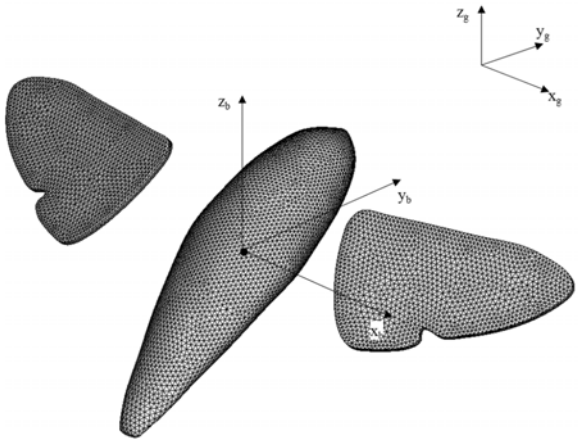


(a)

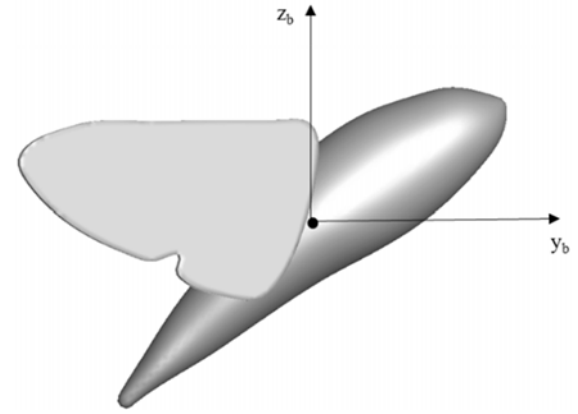


(b)

Fig. 2 Drawing of insect model and coordinate systems: (a) Perspective view with surface mesh. (b) Side view. The longitudinal axis of insect body is selected as the $y_b$ axis of body frame. The insect model is created with a pre-set pitch angle of 45° in the body frame

$$\partial_t \mathbf{u} = -(\mathbf{u} - \mathbf{u}^g) \cdot \nabla \mathbf{u} + \frac{1}{\mathrm{Re}} \Delta \mathbf{u} - \nabla p \tag{3}$$

where $\mathbf{u}(\mathbf{x}, t)$ and $p(\mathbf{x}, t)$ represent the velocity and pressure fields of the fluid domain respectively. The $\mathbf{u}^g$ is the convection velocity of the computational node, which is equal to zero for stationary nodes.

The governing equations are solved on a hybrid background Cartesian grid nodes and clouds of meshfree grids around IBs. The standard 7-point central finite difference scheme is applied at Cartesian nodes that do not have meshfree nodes nearby, while the SVD-GFD scheme is applied at the meshfree nodes and Cartesian nodes with meshfree nodes nearby. A second-order implicit projection method, based on a fractional-step Crank-Nicolson scheme is applied here to solve the ALE form NS equations. Detail of this method has been discussed by [7] and [9], which will not be elaborated here.

The flyer is located in a cubic domain with boundaries set at a distance of about three wing lengths away from the flyer. The grid is non-uniform with coarse grid on the outside and fine grid

near the centre where the model insect is located to give good resolution to the immediate flow around the flyer.

Considering the flapping wing flyer with mass ***M*** as one rigid body, and denoting the linear and angular velocities at its centre of mass ***C*** as $\mathbf{V}_C(t)$ and $\boldsymbol{\omega}(t)$ respectively, the governing dynamical equations for the flyer are then given by

$$\begin{aligned}
&\frac{\mathrm{d}\mathbf{X}_C(t)}{\mathrm{d}t} = \mathbf{V}_C(t) \\
&\frac{\mathrm{d}\boldsymbol{\Theta}(t)}{\mathrm{d}t} = \left[\mathbf{K}(\boldsymbol{\Theta})\right]\cdot\boldsymbol{\omega}(t) \\
&\frac{\mathrm{d}(M\cdot\mathbf{V}_C)}{\mathrm{d}t} = -Mg\mathbf{i}_z + \int_{\Gamma(t)}\left[\boldsymbol{\sigma}\right]\cdot\mathbf{n}d\Gamma \\
&\frac{\mathrm{d}\left(\left[\mathbf{I}(t)\right]\cdot\boldsymbol{\omega}(t)\right)}{\mathrm{d}t} = \int_{\Gamma(t)}\left(\mathbf{x}-\mathbf{X}_C(t)\right)\times\left(\left[\boldsymbol{\sigma}\right]\cdot\mathbf{n}\right)d\Gamma
\end{aligned} \tag{4}$$

$\mathbf{X}_C(t)$ is the location of CoM at time $t$. $\boldsymbol{\Theta}(t)$ is the rotation angle vector of the flyer. $[\mathbf{K}(\boldsymbol{\Theta})]$ is a transformation matrix, which transforms the angular velocity $\boldsymbol{\omega}(t)$ of the flyer into the rate of change of its orientation vector $\boldsymbol{\Theta}(t)$. $[\boldsymbol{\sigma}]$ is the Newtonian fluid stress tensor which can be obtained from CFD solver. $[\mathbf{I}(t)]$ is the inertia tensor of the flyer, $\Gamma$ denotes the surface of the rigid body and $\mathbf{x}$ denotes the location of an arbitrary point on the surface. More details about the fluid dynamics and fluid-body interaction involved in the research can be found in [6].

## III. Flight Control

An insect has 6 degrees of freedom in total when it flies; they are surge (forward/backward), heave (up/down), sway (left/right), roll, yaw and pitch. Surge, heave and pitch are grouped together as longitudinal motion, and the remaining three are grouped as lateral motion. Since the longitudinal motion and lateral motion are usually coupled weakly, they can be analysed separately. In this paper, only the longitudinal flight is investigated.

The stroke-plane adjustment can be used to control the trust forces and pitch moment generated by the wing pair, and thus to control the longitudinal motion. The adjustments of stroke-plane are done by rotation the wing frame around the affixed wing roots. Small pitching rotation of the stroke plane can generate horizontal forces ($y$-direction) to control the forward/reverse motion of the flyer (Fig. 3). For the hovering flight, the disturbance in the mean lift force and mean thrust are generally quite small. Hence, relatively small rotations of the stroke plane are needed to neutralize or counter them. This means that subtle modulation of the wingbeat frequency $f$ will be normally be sufficient to moderate changes in the net vertical force during hovering. Biasing the stroking action of the wings in the stroke plane can shift the cycle-averaged centre of the wing force, and generate desired moment to counter the pitching disturbance of the flyer. The described stroke-plane adjustment thus comprises three independent controlling actions: pitching rotation of stroke plane ($\beta$), biasing the mean positional angle of the wing stroke ($\gamma$) and wingbeat frequency ($f$) modulation. The orientation of wing frame and wingbeat frequency is updated at the beginning of each wingbeat. If the orientation of wing frame is changed, sixth order polynomials will be used to describe the rotation of wing frame from old orientation to the new one within one wingbeat.

A generic PID based feedback control algorithm is used in the present study. All the variables are controlled independently in both the stroke-plane adjustments and intra-stroke adjustments. The PID feedback control system comprises three components: a proportional component P that reflects the current deviation (also termed the error) from the desired state, an integral component, I, that takes into account recent error events, and a differential component, D, for estimating likely future error based on the current rate of deviation/error change. The correction or control vector that it works out is a weighted combination of these three components to give

$$\mathbf{u}(t) = K_P\mathbf{e}(t) + K_I\int_0^t\mathbf{e}(\tau)\mathrm{d}\tau + K_D\frac{\mathrm{d}}{\mathrm{d}t}\mathbf{e}(t) + \mathbf{u}(0) \tag{5}$$

More details about the flight control involved in the research can be found in [6].

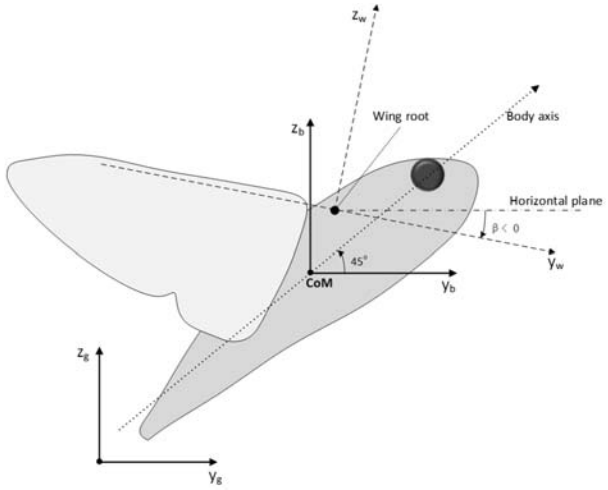


Fig. 3 Orientation of wing frame/stroke-plane: The wing stroke-plane forms an angel $\beta$ (stroke plane angle) with respect to horizontal when the insect is viewed laterally

## IV. Effect of Control Actions

Fixed body simulation with prescribed wing flapping motion is conducted to analyse the effect of different control actions. Mean positional angle ($\gamma$), wing plane angle ($\beta$) and wing beating frequency ($f$) are varied to study how the force and torque acting on the insect are changed. The results are summarized in Figs. 4-6. It can be found that the effects of $\gamma$ and $f$ are unique, the former one varies the pitching torque only and the latter one aims to change the vertical force. However, the wing plane angle ($\beta$) can change both the longitudinal force and pitching torque, the latter one of which is undesired. To remove such effect, we need to add one more

term to the final mean positional angle, in additional to the PID controller output.

$$\gamma = \gamma_{PID} - k\beta \quad (6)$$

$k \approx 0.3$, which is the ratio of the gradients in Figs. 5 (f) and 4 (b). In such way, each control parameter takes care of one degree of freedom independently, where the insect flight is easier to control.

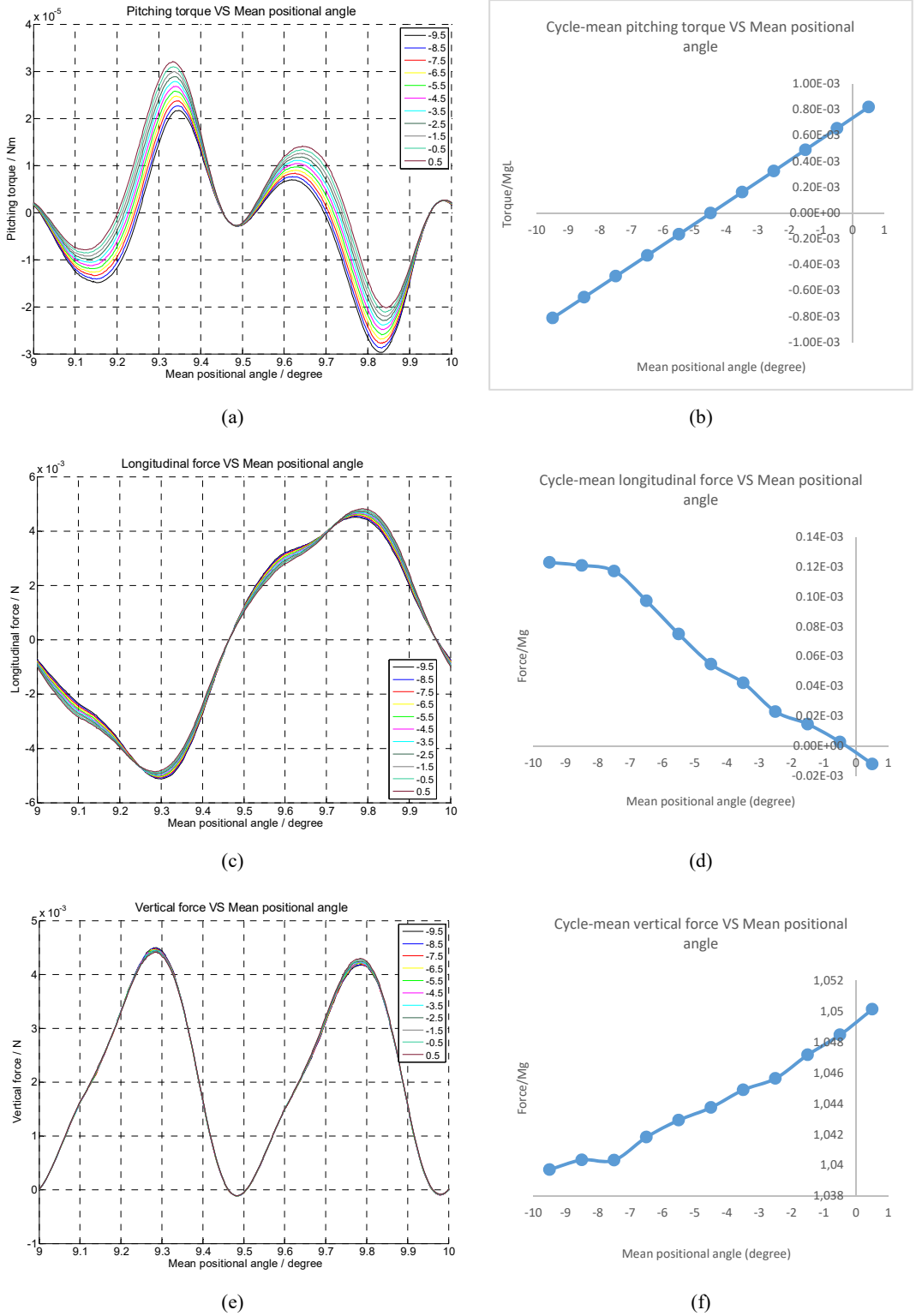


Fig. 4 Effect of mean positional angle: It mainly changes the pitching torque, which varies linearly near the equilibrium position; Change of the vertical force and longitudinal force is within 2%

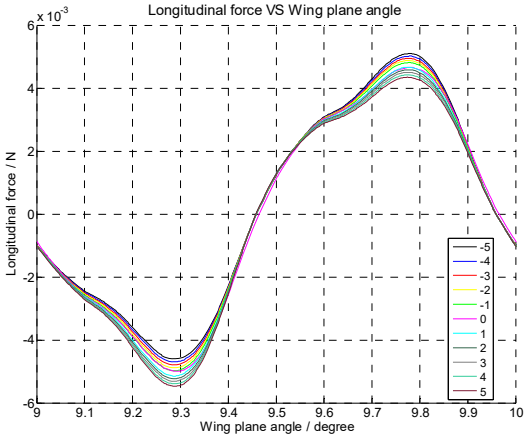


(a)

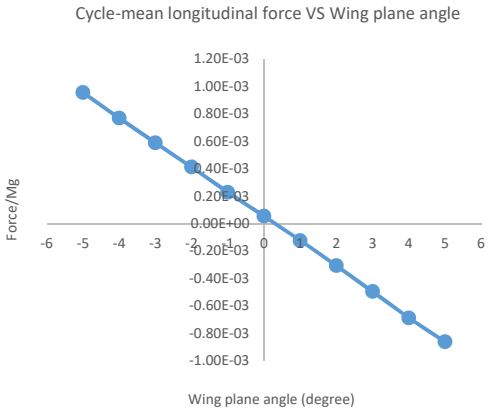


(b)

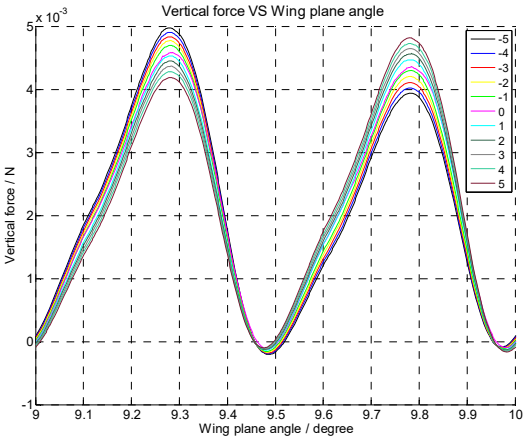


(c)

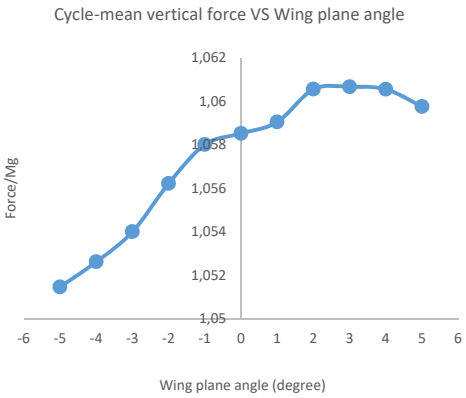


(d)

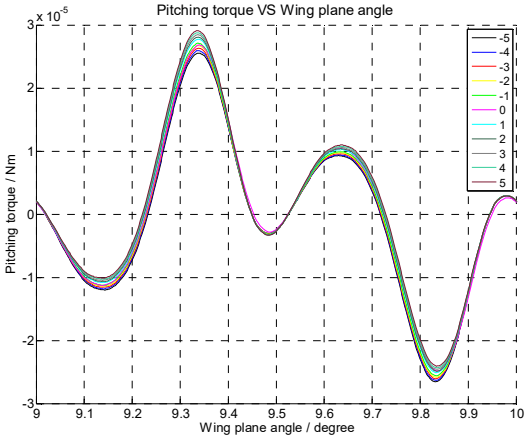


(e)

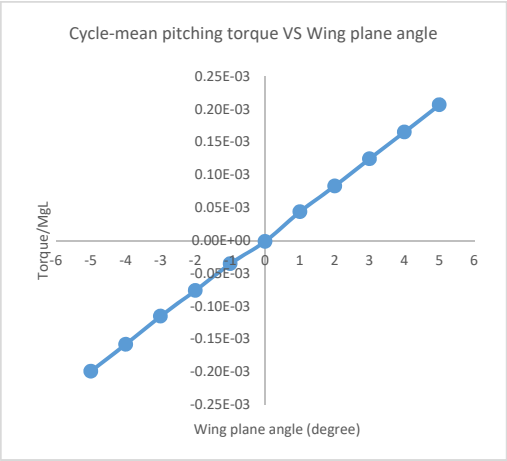


(f)

Fig. 5 Effect of wing plane angle: It changes the longitudinal force and pitching torque, both of which vary linearly near the equilibrium position; Change to the vertical force is negligible

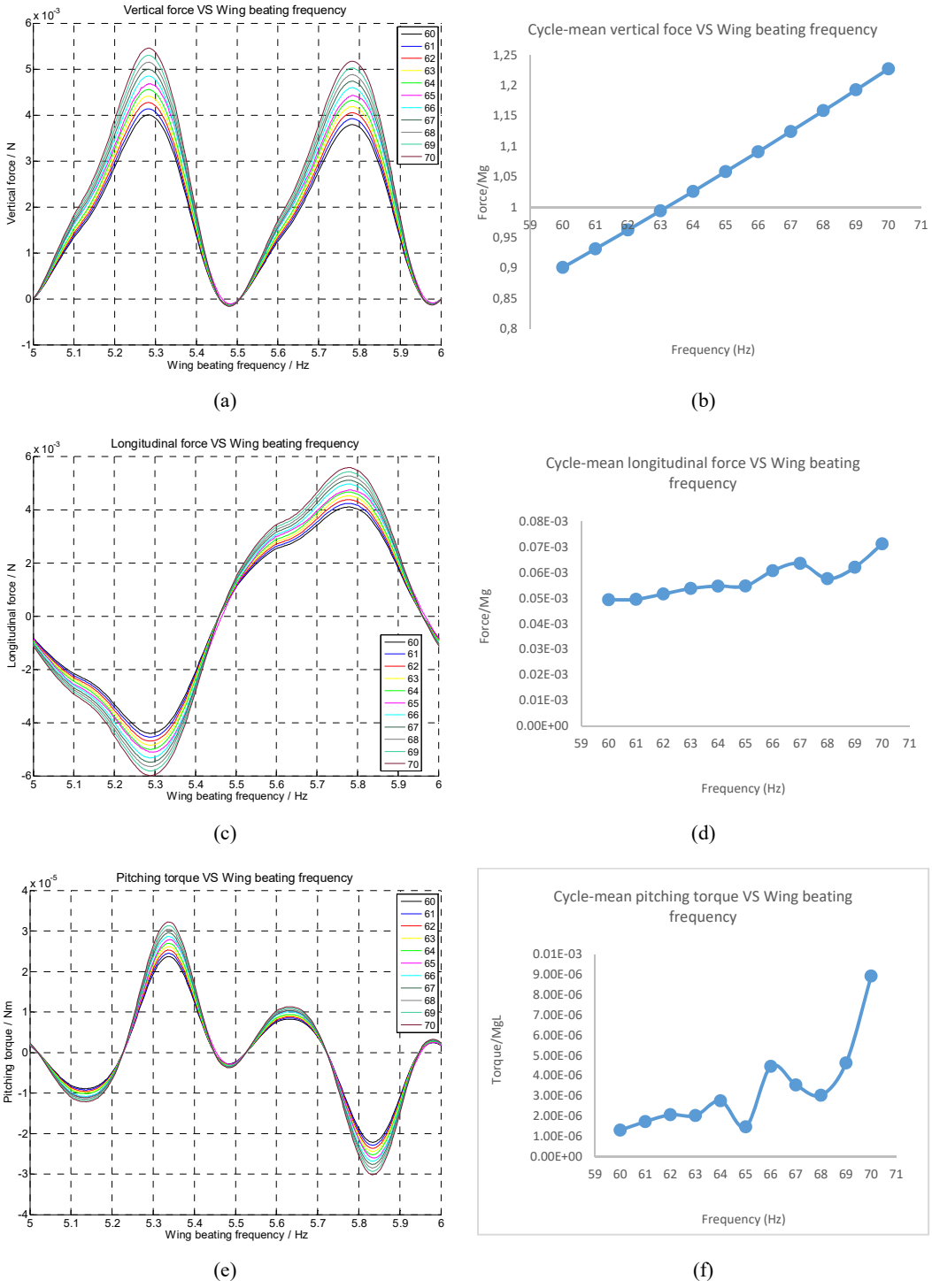


Fig. 6 Effect of wing beating frequency: It mainly changes the vertical force, which varies linearly near the equilibrium position; Change of the pitching torque and longitudinal force is nonsignificant

## V. Controlled Hovering Flight

The PID controller is carefully tuned in each degree of freedom, the insect hovering flight can be well controlled.

Figs. 7 and 8 show the hovering behaviour of the model hummingbird hawkmoth over a period of 50 wing cycles. The simulation shows how the body oscillate during hovering, which is an expected phenomenon due to the cyclical nature of the aerodynamic forces and moment. The action of the controller to sustain hovering at the designated position and attitude is shown in Figs. 9 and 10. It can be found that the amplitude of pitch oscillation is controlled within 10 degrees for the overall simulation and is within 5 degrees for one whole oscillation when the flight is stabilized in the end. The pitch oscillation is in a reasonable range compared to the real

hummingbird hawkmoth [10]. In addition, the position of the insect is kept in close vicinity of the designated location, to be more specific, within the range of 15 percent of the wing length. Overall, the control coefficients are able to make the insect hover with good performance.

When the insect starts to drift backward and pitch upward at the beginning of the simulation, the controller tries to restore the insect to the designated status by increasing the forward force and pitching down torque. That is done by pitching the stroke plane forward (downward) and rotating the mean positional angle backward. Simultaneously, the insect moves upward slightly at the beginning and it is brought back by the controller by reducing the wing beating frequency, which in turn decreases the lift. It can be deduced from the controller record that the currently used PID controller is very responsive and can make the insect hover well. Furthermore, the average mean positional angle is around -4.5 degree, that is to say, the symmetric axis of the wing motion has to be swept backward by -4.5 degree so that the acting point of the mean lift force is just above the CoM. The wing beating frequency change very little during the hovering, as shown by Figure 10. The reason is that small change in frequency is enough to correct for lift deficiency.

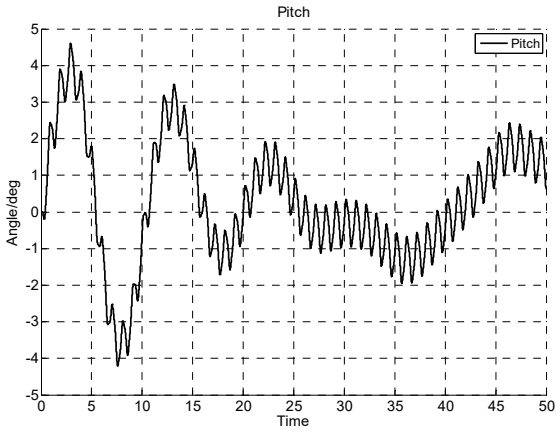


Fig. 7 Evolution of pitch angle during hovering

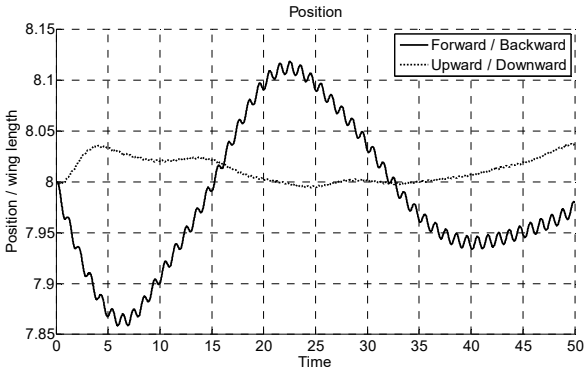


Fig. 8 Trajectory of CoM during hovering

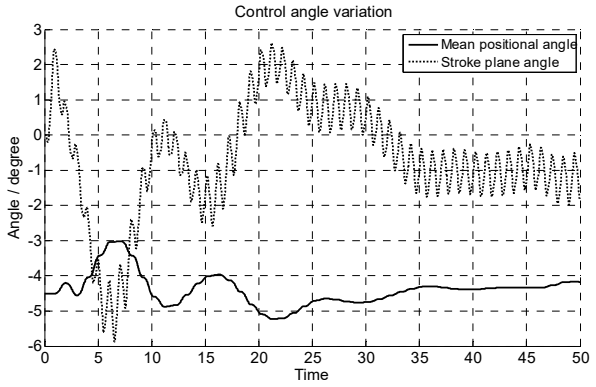


Fig. 9 Variations of stroke plane angle $\beta$ and mean positional angle $\gamma$

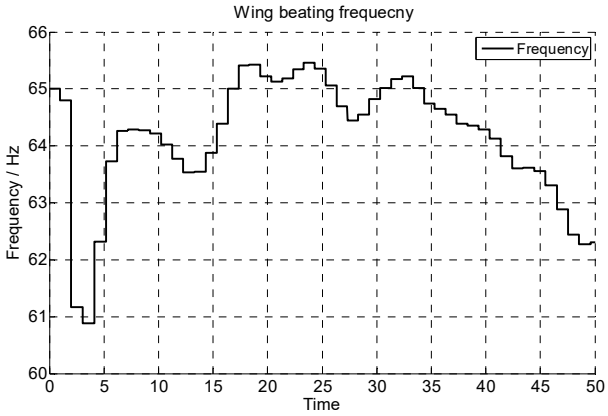


Fig. 10 Evolution of wing beating frequency

## VI. Conclusion

In the present study, the SVD-GFD based CFD solver is adapted to study the dynamics of a free hovering flapping-wing flyer. A complex irregular shaped body and wings of the hummingbird hawkmoth has been modelled with rigid wing assumptions. The PID controllers are established to achieve the designated flight. The controllers are proven to be robust and effective at adjust the wing kinematics to stabilize the flyer and control the direction of normal hovering flight. The present modelling approach offers a promising route of investigation that could complement as well as overcome some of the limitations of experiments in the area of free flight aerodynamics of insects. Study shows that the hummingbird hawkmoth is able to hover with reasonable pitch amplitude and very small displacement from the designated location. The PID control mechanism is shown to be stable and responsive to make the hummingbird hawkmoth hover.

## References

[1] Ellington, C.P., et al., Leading-edge vortices in insect flight. 1996.
[2] Brodsky, A., Vortex formation in the tethered flight of the peacock butterfly *Inachis io* L. (Lepidoptera, Nymphalidae) and some aspects of insect flight evolution. Journal of experimental biology, 1991. 161(1): p. 77-95.
[3] Lua, K., et al., On the aerodynamic characteristics of hovering rigid and flexible hawkmoth-like wings. Experiments in fluids, 2010. 49(6): p. 1263-1291.

[4] Sun, M. and J. Tang, Unsteady aerodynamic force generation by a model fruit fly wing in flapping motion. Journal of Experimental Biology, 2002. 205(1): p. 55-70.
[5] Miller, L.A. and C.S. Peskin, A computational fluid dynamics of clap and fling' in the smallest insects. Journal of Experimental Biology, 2005. 208(2): p. 195-212.
[6] Wu, D., K. Yeo, and T. Lim, A numerical study on the free hovering flight of a model insect at low Reynolds number. Computers & Fluids, 2014. 103: p. 234-261.
[7] Chew, C.S., K. Yeo, and C. Shu, A generalized finite-difference (GFD) ALE scheme for incompressible flows around moving solid bodies on hybrid meshfree–Cartesian grids. Journal of Computational Physics, 2006. 218(2): p. 510-548.
[8] Wang, X., et al., A SVD-GFD scheme for computing 3D incompressible viscous fluid flows. Computers & Fluids, 2008. 37(6): p. 733-746.
[9] Yu, P., et al., A three-dimensional hybrid meshfree-Cartesian scheme for fluid–body interaction. International Journal for Numerical Methods in Engineering, 2011. 88(4): p. 385-408.
[10] Wu, G. and L. Zeng, Measuring the kinematics of a free-flying hawk-moth (*Macroglossum stellatarum*) by a comb-fringe projection method. Acta Mechanica Sinica, 2010. 26(1): p. 67-71.